https://doi.org/10.17221/42/2023-SWR

Temporal variation in soil rill erodibility and critical shear stress during concentrated flow for three different crops

Ke-Lin Chen[1], Yun-Fei Yan[1], Yi-Heng Li[1], Heng Zhang[1], Ke-Ming Tang[1,2], Huai-Yu Wu[2], Yi-Yang Kang[2]*

[1]*College of Water Conservancy and Hydropower Engineering Sichuan Agricultural University, Agricultural Water-Soil Engineering, Sichuan Agricultural University, Ya'an, P.R. China*
[2]*College of Water Conservancy and Hydropower Engineering Sichuan Agricultural University, Hydraulic and Hydro-Power Engineering, Sichuan Agricultural University, Ya'an, P.R. China*

**Corresponding author: ckl242243@163.com*

Citation: Chen K.L., Yan Y.F., Li Y.H., Zhang H., Tang K.M., Wu H.Y., Kang Y.Y. (2023): Temporal variation in soil rill erodibility and critical shear stress during concentrated flow for three different crops. Soil & Water Res., 18: 181–191.

Abstract: Soil rill erodibility (K_r) and critical shear stress (τ_c) are important parameters in some physical soil erosion models. In the present study, the temporal variations in K_r and τ_c by overland flow were investigated using undisturbed topsoil samples collected from three cropped plots (ryegrass, lucerne, and corn) and a fallow plot. In this study, the potential factors leading to these changes were examined from March to September 2022 in western Sichuan Province, China. The results revealed significant seasonal variations in K_r, τ_c, soil bulk density (SD), soil cohesion (SC), and soil water-stable aggregate (WSA). The K_r values were significantly lower, whereas τ_c values were slightly higher for cropped plots when compared to that for the fallow plot. The mean K_r values for cropped plots were 4.51~17.26 times lower than that for the fallow plot. In contrast, the mean τ_c values for the cropped plots were 1.03~1.08 times higher than that for the fallow plots. The results also indicated a negative correlation of K_r with SD, SC, WSA, soil organic matter content (SOC), and root weight density (RWD), while a positive correlation of τ_c with SD, SC, WSA, and RWD. Furthermore, an exponential decrease in K_r was observed with an increase in SD, SC, WSA, SOC, and RWD. An increase in SD, SC, WSA, and RWD of the experimental plots led to a further increase in τ_c.

Keywords: root weight density; soil bulk density; soil cohesion; soil organic matter content; soil water-stable aggregate

Soil erosion has become a severe problem, affecting the global ecosystem and sustainable agricultural development (Zhao et al. 2013; Amundson et al. 2015; Keesstra et al. 2016). Soil erosion leads to soil degradation and loss of arable land, which has a negative effect on land productivity (Li & Fang 2016; Zhang et al. 2019a). Further, contaminants in the migrating soil sediments could enter water resources and lead to water pollution (Wang et al. 2017).

Based on different erosion forces, soil erosion can be divided into water erosion, wind erosion, freeze-thaw erosion, etc. Soil rill erosion is a common type of water erosion observed in western Sichuan Province, China. Soil rill erodibility (K_r) and critical shear stress (τ_c) were considered essential parameters in the Water erosion prediction project (WEPP) model for characterising the soil erosion resistance (Knapen et al. 2007b). K_r and τ_c reflect the susceptibility and sensitivity of soil to denudation and transport by external forces, respectively. These parameters are the intrinsic factors affecting soil loss and the basis for the quantitative study on soil erosion. Soil rill erosion primarily occurs at the soil surface. Therefore, K_r and τ_c are predominantly influenced by the physicochemical properties of the soil, such as soil water-stable aggregate (Zhang et al. 2019b), soil organic matter content (Wang et al. 2014a), soil bulk density (Wang et al. 2015), soil cohesion (Wang

https://doi.org/10.17221/42/2023-SWR

et al. 2018) and plant root growth (Bennett et al. 2000; Mamo & Bubenzer 2001a, b).

Good soil structure has a positive influence on soil erosion resistance. Soil bulk density (SD), soil cohesion (SC), and soil water-stable aggregate (WSA) are key indicators of the soil structure. SD and SC indicate the compactness of soil particles, which directly affects the soil erosion resistance (Zhang et al. 2019a), while WSA is closely associated with the soil ecosystem processes such as soil nutrient sequestration, water retention, and soil erosion (Six et al. 2000; Borrelli et al. 2017). The stability of soil aggregates affects water, fertiliser, air, and heat in the soil and directly influences soil erodibility (Zhou et al. 2012). De Baets et al. (2006) demonstrated that the soil structure is primarily influenced by soil organic matter content (SOC) and root growth. SOC is one of the important parameters for effectively improving soil physicochemical properties (Minasny et al. 2017). Soil organic matter accumulation is crucial for improving internal stability and ground strength. In addition, it plays a major role in maintaining soil quality. Soil organic matter consists of humus and other cementing substances that promote the formation of macroparticles as well as improve soil structure. It can also act as an energy source for the growth of soil microorganisms and animals. Soil organic matter provides nutrients for plant growth after decomposition and promotes the growth of plant root, which, in turn, positively impacts the soil structure and improves soil resistance to erosion (Gyssels et al. 2005; Wen et al. 2017).

Plant affects soil erosion by reducing the damage caused by the direct impact of raindrops on soil particles. On the other hand, the growth of plant roots improves the soil structure and enhances the ability of the soil to resist dispersion, suspension, and transport of soil particles caused by runoff. Thus, improvement in soil erosion resistance by well-developed plant roots is the primary mechanism by which the plants affect soil erosion. Seasonal changes affect soil physicochemical properties and root growth activities, while soil rill erosion is affected by the changes in soil physicochemical properties and root growth activities (Gyssels et al. 2005; Maetens et al. 2012; Stokes et al. 2014; Wang et al. 2015; Sun et al. 2016; Zhang et al. 2019b; Bordoloi & Ng 2020). However, different vegetation has varying root growth trends, and the seasonal variation in soil erosion resistance caused by root growth activities is also different. However, there is a lack of information on the effects of seasonal variation effects of different plant communities on soil erosion resistance. Corn is the major food crop in western Sichuan. In addition, excellent forage grasses, such as ryegrass and lucerne, are widely grown in pasture areas. Corn has a fibrous root system containing several branches, dense root hairs, and large roots. In contrast, the ryegrass root system is characterised by short rhizomes and dense fibrous roots, while lucerne is characterized by developed and thick roots.

The objectives of this study are: (a) to investigate the effects of ryegrass, lucerne, and corn on SD, SC, WSA, SOC, K_r, and τ_c; (b) to determine the temporal dynamics of SD, SC, WSA, SOC, root weight density (RWD), K_r and τ_c under different crops; and (c) to examine the potential relationships between soil parameters (SD, SC, WSA, SOC, and RWD) with K_r and τ_c. The findings of this study will be useful in understanding the soil erosion mechanism and water conservation requirements in this region.

MATERIAL AND METHODS

Study area. The experimental field plots were located at the Scientific Research Base of Sichuan Agricultural University, Ya'an City, Sichuan Province, China (29°58'10''N,102°59'14''E). The climate is subtropical monsoonal with significant vertical changes in temperature and low annual total solar radiation. The study region has an annual average temperature of 16.5 °C and annual rainfall of 1 750 mm. The rainfall distribution is uneven throughout the year, with most of the rainfall occurring between May and October, with June~August receiving the highest amount of rainfall. The annual evaporation is 838.8 mm, and the soil type is purplish soil. The experimental plots have flat slopes.

Experimental design and sample collection. The crops selected for the current study were ryegrass (R), lucerne (L), and corn (C), while the fallow plot (CK) was bare land without crops. The dimension of each plot was 10 × 3 m. Before the collection of soil samples, all experimental plots were tilled by mouldboard plough to a depth of 15~20 cm, and plant residues were removed. Then, the ryegrass and lucerne plots were sown in strips at a density of 2.24 g/m^2, and the corn was sown into rows with a distance of 30 cm on 25 March. No weeding was required in the R and L plots, while herbicides were used for the C and CK plots to remove weeds once a month. The experiment started in late March

https://doi.org/10.17221/42/2023-SWR

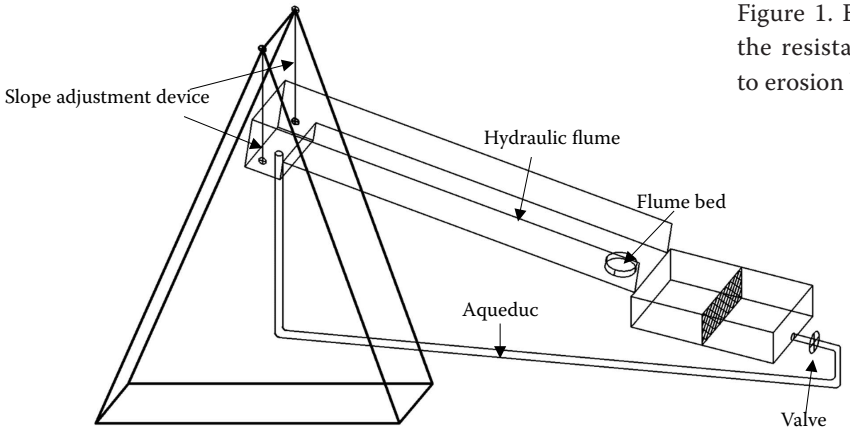

Figure 1. Experimental set-up used for testing the resistance of undisturbed topsoil samples to erosion by concentrated flow

and ended in late September 2022. Soil sampling was carried out at an interval of approximately 30 days. Soil detachment capacity, soil bulk density, soil cohesion, soil water-stable aggregate, soil organic matter content, and root weight density were measured. The testing of soil samples for soil bulk density, soil cohesion, soil water-stable aggregate, soil organic matter content and root weight density was performed in triplicates, while the soil detachment capacity test was in quintuplicate.

A total of thirty undisturbed soil samples were collected from each plot per cycle with a steel ring (10 cm inner-diameter and 5 cm inner-height) for the measurement of soil detachment capacity. Before sampling, a scissor was used to carefully cut off vegetation at ground level. Then the steel ring was slowly pushed into the soil, and the soil around the ring was removed with a knife to minimise disturbance to the core. The amount of soil collected by each steel ring should be enough to fill the ring and flush with the top and bottom edges of the ring. Further, the sample was slowly turned over to remove the excess soil. The soil surface was covered with two cotton pads, and the top and bottom covers of the sample were correctly placed over them. Before flushing, the soil samples were soaked in water for 12 h to ensure consistent soil water saturation. Then the wet soil samples were shade dried for 3 h, and the flushing experiments were conducted. The soil samples were carefully and immediately placed into the bottom hole of the flume for scouring under the designed hydraulic conditions. When the scour depth of the soil sample is about 2 cm, the test is stopped to eliminate the potential influence of the flow turbulence generated by the scour depth on the measured soil detachment capacity. The remaining wet soil samples were dried at 105 °C for 24 h and weighed to calculate the final dry mass.

The soil water-stable aggregate was measured by the wet-sieving method. Soil bulk density was measured by the oven-drying method. Soil cohesion was measured using a pocket torvane. Soil organic matter content was determined by the potassium dichromate volumetric method-external heating method. After scouring, the soil samples were collected to measure the RWD using the weighing method.

Soil detachment capacity measurement and soil resistance fitting. Soil detachment capacity was determined using a variable slope test flume system (flume length 5 m, width 0.4 m, and height 0.3 m) (Figure 1) at five different flow shear stresses produced by different combinations of slope gradients (ranging from 8.75 to 36.39%) and flow discharges (ranging from 1 to 3 L/s) (Table 1).

The flow shear stress (τ) was calculated using Equation (1) (Nearing et al. 1989).

$$\tau = \rho g H S \quad (1)$$

where:

ρ – the water density (kg/m^3);

g – the acceleration of gravity (m/s^2);

H – the flow depth (m);

S – the slope (%).

Table 1. Slope flow hydraulics parameters in the test

Slope (%)	Flow discharge (L/S)	Flow shear stress (Pa)
8.75	1	3.63
17.63	1	6.13
26.79	2.5	10.49
26.79	2.5	13.80
36.39	3	17.83

https://doi.org/10.17221/42/2023-SWR

The soil detachment capacity (*Dc*) was calculated using Equation (2) (Nearing et al. 1989):

$$Dc = \frac{W_a - W_b}{t \times A} \quad (2)$$

where:

W_a – the dry weight of soil in the ring (kg) before the detachment test (the difference between the original weight of the wet soil sample and the water content);

W_b – the dry weight of soil in the ring after the detachment test (kg);

t – the detachment test period (s);

A – the cross-section area of the sample (m^2).

K_r and τ_c are calculated using the simplified equation of the WEPP model (Nearing et al. 1989) as given by Equation (3).

$$Dc = K_r(\tau - \tau_c) \quad (3)$$

where:

K_r – soil rill erodibility (s/m);

τ_c – the critical shear stress (Pa).

Data analysis. A one-way ANOVA followed by Duncan's test was used to compare the differences in influencing factors of the same crop at different periods. The correlations between K_r and τ_c, and all the influencing factors were determined by Pearson correlation analysis. Independent-sample test (*t*-test) was employed to detect differences plots in K_r of different plots. Non-linear regression was applied to evaluate the relationships between K_r, τ_c and all influencing factors (SD, SC, WSA, SOC and RWD). All the statistical analyses were conducted using SPSS Statistics (Ver. 25.0).

RESULTS AND DISCUSSION

Temporal variation in soil rill erodibility and critical shear stress

Soil rill erodibility. The temporal variation in K_r observed from different study plots is shown in Figure 2A. K_r initially increased and then decreased in all plots (R, L, C and CK) from March to May. K_r values were nearly constant in the cropped plots (R, L and C) from May to September. However, in the case of CK, a further decrease in K_r was observed from May to September. Wide variations in K_r were observed in the L plot, followed by C, R, and CK plots from April to September. The ratios of maximum to minimum K_r were 7.94, 17.59, 26.72, and 3.37 for the R, L, C, and CK plots, respectively. Similarly, the coefficients of variation for K_r were 1.04, 1.55, 1.72, and 0.58 for R, L, C, and CK plots, respectively. This study demonstrated less variability in K_r of R than that of L and C during the period of measurement in the region. Significant differences were observed between CK and cropped plots. However, the independent-sample t-test indicated no significant difference in K_r among the R, L, and C plots (Table 2). A significant increase was observed in the K_r value of R, L, C, and CK plots in the first month after tillage, which was 8.33, 44.40, 30.89, and 65.69 times the K_r value before tillage, respectively. Tillage

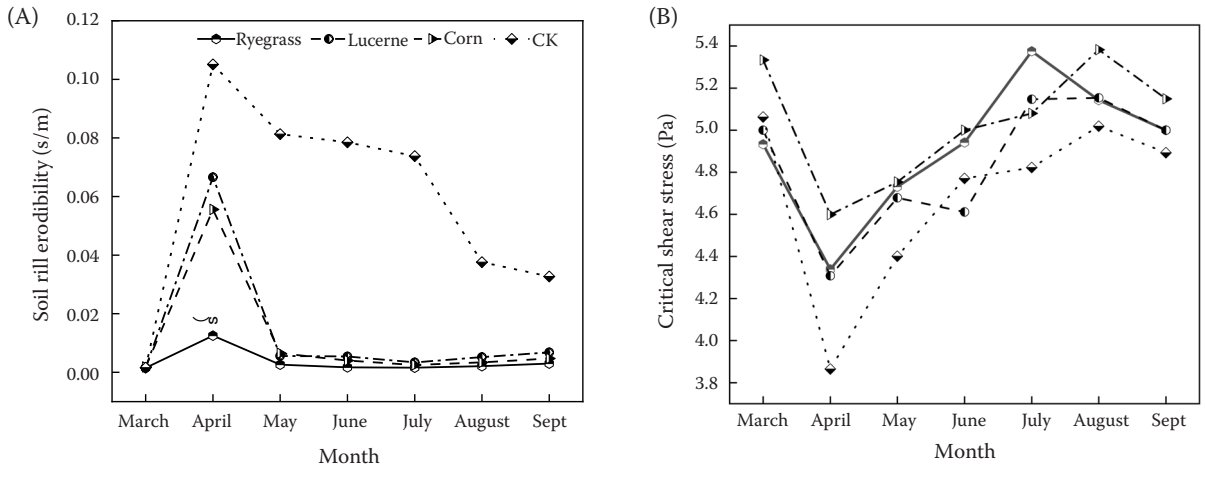

Figure 2. Temporal variation of soil rill erodibility (A) and of critical shear stress (B)
CK – control

https://doi.org/10.17221/42/2023-SWR

Table 2. Dependent *t*-test for paired samples

Pair	SD	SEM	*t*	df	Significance
1 CK-R	0.343	0.129	4.261	6	0.005
2 CK-L	0.282	0.107	4.348	6	0.005
3 CK-C	0.281	0.106	4.338	6	0.005
4 L-R	0.169	0.064	1.399	6	0.211
5 C-L	0.032	0.012	0.240	6	0.819
6 C-R	0.198	0.075	1.230	6	0.265

C – corn; L – lucerne; R – ryegrass; CK – control; SD – standard deviation; SEM – standard error of mean; *t* – significance test; df – degree of freedom

practices decreased resistance to soil erosion in all plots. The K_r values decreased by 79.20, 91.59, 88.31, and 22.65% in R, L, C, and CK plots, respectively from April to May. The decline in K_r was attributed to soil consolidation and the growth of plant root systems. The K_r values for the R, L, and C plots were found to be nearly constant after May. The mean K_r values for the R, L, and C plots were significantly lower (16.42, 4.35, and 5.23 times lower) than that for the CK plot, respectively. The mean K_r value for the R plot was 0.27 and 0.32 times than those for the L and C plots, respectively. In the experimental plot of R, the growth of several fine and delicate white roots on the surface was observed, which could improve the resistance to soil erosion. Therefore, the K_r of the R plot was slightly lower than that of the C and L plots. Further, the K_r value for the R, L, and C plots were 0.18, 0.63, and 0.64 times higher than the WEPP reference value (0.02 s/m) (Alberts et al. 1995), respectively, which could be due to inherent soil characteristics and type of plant species.

Critical shear stress. The temporal variations in τ_c of study plots (R, L, C, and CK) are shown in Figure 2B. τ_c initially decreased and later increased in all the plots from March to September. An increase of 15.25, 16.07, 11.96, and 26.60% were observed in τ_c of the R, L, C, and CK plots, respectively, from April to September. In April, the minimum τ_c values for the R, L, C, and CK plots were 4.34, 4.31, 4.59, and 3.87 Pa, respectively. The maximum τ_c value for the R plot (5.38 Pa) was observed in July, while those for the L (5.15 Pa) and C (5.02 Pa) plots were observed in August. CK plot attained the maximum τ_c value of 5.06 Pa in March. The mean τ_c values for R, L, and C plots were 4.92, 4.84, and 5.04, which were 1.05, 1.03, and 1.08 times higher than that for the CK plot (4.69 Pa), respectively. Wang et al. (2014b) reported a mean τ_c value of 4.38 Pa, which was 12.33, 10.50, and 15.07 times lower than those for the R, L, and C plots, respectively. These differences in τ_c may be attributed to inherent soil characteristics and methods chosen for measuring τ_c. Further, the τ_c values ranged between 4.54~22.54 Pa for flow shear stress in a previous study by Wang et al. (2014b), whereas the τ_c values ranged between 3.63~17.83Pa in the present study.

Factors affecting the temporal variation in soil rill erodibility and critical shear stress

Previous studies have demonstrated that physico-chemical properties of soil such as SD, SC, WSA, SOC and plant root growth influence K_r and τ_c values (Bennett et al. 2000; Knapen et al. 2007a; Wang et al. 2014a, 2015, 2018; Yu et al. 2014; Sun et al. 2016; Zhang et al. 2019b). In this study, K_r and τ_c exhibited a correlation with SD, SC, WSA, SOC, and RWD (Table 3).

K_r and τ_c are influenced by SD. However, in this study, no significant non-linear relationship was

Table 3. Correlation analysis table of each indicator

	K_r	τ_c	SD	SC	WSA	RWD	SOC
K_r	1	–0.692**	–0.507**	–0.812**	–0.740**	–0.458*	–0.459*
τ_c	–0.692**	1	0.565**	0.778**	0.662**	0.443*	0.194

K_r – soil rill erodibility; τ_c – critical shear stress; SD – bulk density; SC – soil cohesion; WSA – water-stable aggregate; RWD – root weight density; SOC – soil organic matter content; *, **indicate a significant correlation at the 0.05 and 0.01 level; n = 24

https://doi.org/10.17221/42/2023-SWR

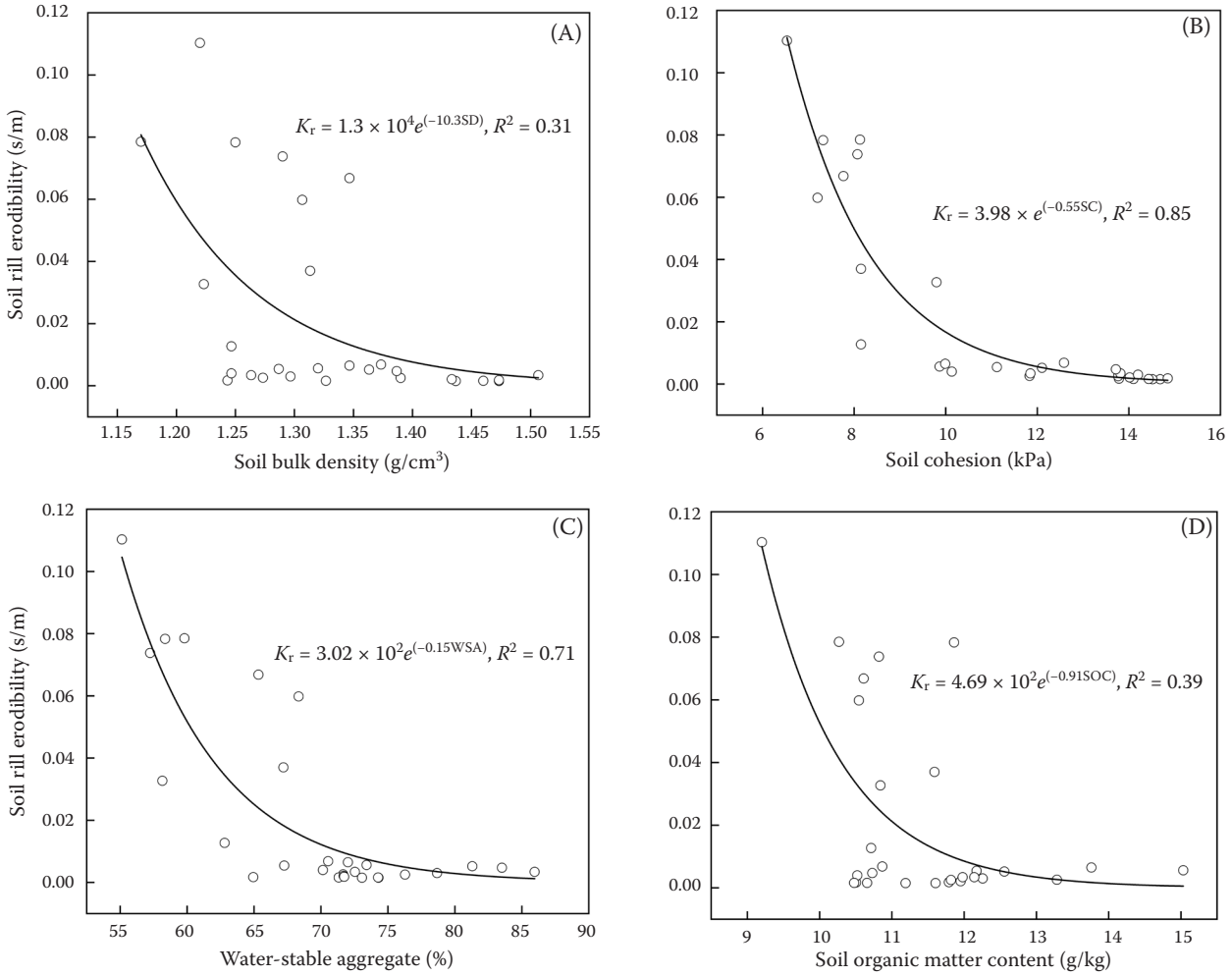

Figure 3. Soil rill erodibility (K_r) as function of soil bulk density (A), soil cohesion (B), water-stable aggregate (C), and soil organic matter content (D)

SD – bulk density; SC – soil cohesion; WSA – water-stable aggregate; SOC – soil organic matter content

observed between SD and K_r (R^2 = 0.31) and τ_c (R^2 = 0.32). An exponential decrease in K_r was observed with an increase in SD (Figure 3A), while an increase in $\boldsymbol{\tau}_c$ with an increase in SD can be expressed as a power function (Figure 4A). The trends observed for K_r and τ_c values were attributed to extreme weather events such as unexpected heavy rainfall (late June) and prolonged extreme dry weather (July to August) occurring in the southwest in the study year, which eventually affects the physicochemical properties of the soil.

SD of the R, L, C, and CK plots increased by 4.01, 5.10, 2.97, and 0.27%, respectively from April to September. The factors such as climate, crop growth cycle, and agricultural tillage practices might influence the exchange of material and energy between crops and the soil, which in turn affects the arrangement of soil particles and changes the structure and properties of the soil (Norris 2005; Virto et al. 2011). The R, L, C, and CK plots had minimum SD of 1.25, 1.26, 1.25 and 1.17 g/cm^3, while the maximum SD values were 1.44, 1.47, 1.57, and 1.46 g/cm^3, respectively, i.e., an increase of 15.20, 16.67, 25.60, and 24.79%, respectively (Figure 5A).

In this study, K_r was found to exponentially decrease with an increase in SC with a coefficient of determination of 0.86 (Figure 3B). This result is consistent with the findings from a previous study by Knapen et al. (2007a). As shown in Figure 4B, the increase in τ_c with the increase in SC can be expressed as a power function. Zhang et al. (2013) also suggested a strong relationship between K_r with SC.

Figure 5B shows the variations in SC of R, L, C, and CK plots from March to September. SC of R,

https://doi.org/10.17221/42/2023-SWR

L, C, and CK plots increased by 74.23, 74.77, 76.61, and 50%, respectively from April to September. The minimum SC values for R, L, C, and CK plots in April were 8.15, 7.20, 7.77, and 6.53 kPa, while the maximum SC values were 14.2, 12.58 and 9.80 kPa in September, respectively. However, the maximum value for the C plot (13.82 kPa) was observed in August (Figure 5B).

WSA is an important indicator of the stability of soil aggregates. The larger value of WSA corresponds to the higher stability of the soil aggregates. K_r exhibited a strong negative correlation with WSA, while τ_c was found to be positively correlated with WSA (Table 3). These results are in agreement with the findings of Sun et al. (2016) and Yu et al. (2014), which further indicated that the temporal variations in K_r and τ_c are closely related to the seasonal variation in WSA. The regression results demonstrated an exponential decrease in K_r and that an increase in τ_c with the increase in WSA can be expressed as a power function (Figure 3C and Figure 4C).

Figure 5C shows that the WSA of R (25.27%), L (3.23%), C (27.83%), and CK (5.49%) plots increased inconsistently during the study period. The variations in WSA values for R, L, C and CK plots ranged between 62.80~78.67, 68.33~81.30, 65.33~85.96, and 55.13~67.19%, respectively.

Soil organic matter is beneficial for the formation of soil aggregates. Moreover, it can control the development of soil crusting (Knapen et al. 2007b; Zhang et al. 2019a). In this study, K_r showed a significant negative correlation with SOC. However, τ_c was not significantly correlated with SOC (Table 3). These results are in accordance with the previous results by Zhen et al. (2015). The reason for no relationship between τ_c and SOC can be attributed to the lack of fertilisation during the experiments, which results in a minimal change in SOC. K_r was exponentially decreased with a decline in soil organic matter content (Figure 3D).

As shown in Figure 5D, wide variations in SOC of R, L, C, and CK plots were observed during the

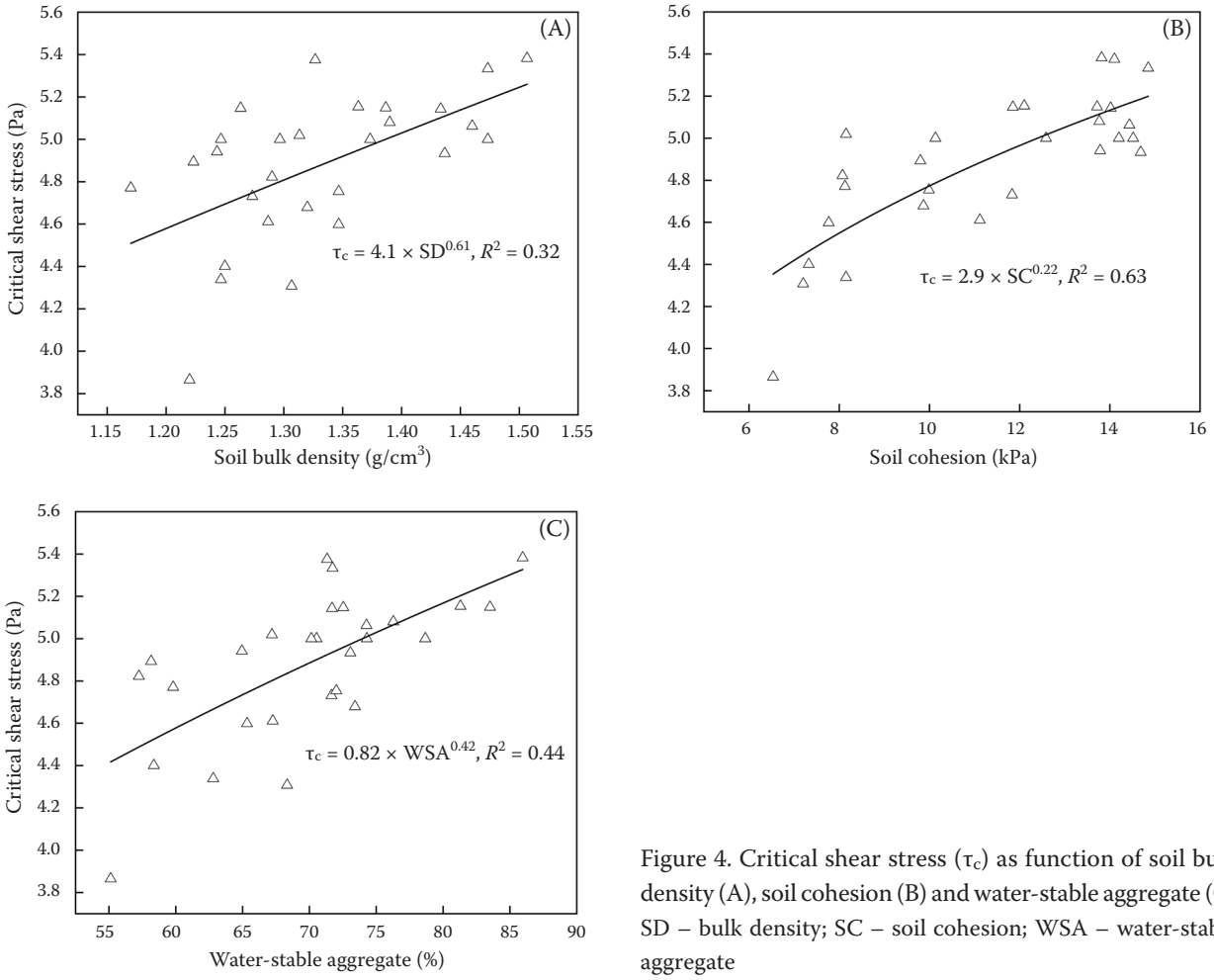

Figure 4. Critical shear stress (τ_c) as function of soil bulk density (A), soil cohesion (B) and water-stable aggregate (C)
SD – bulk density; SC – soil cohesion; WSA – water-stable aggregate

https://doi.org/10.17221/42/2023-SWR

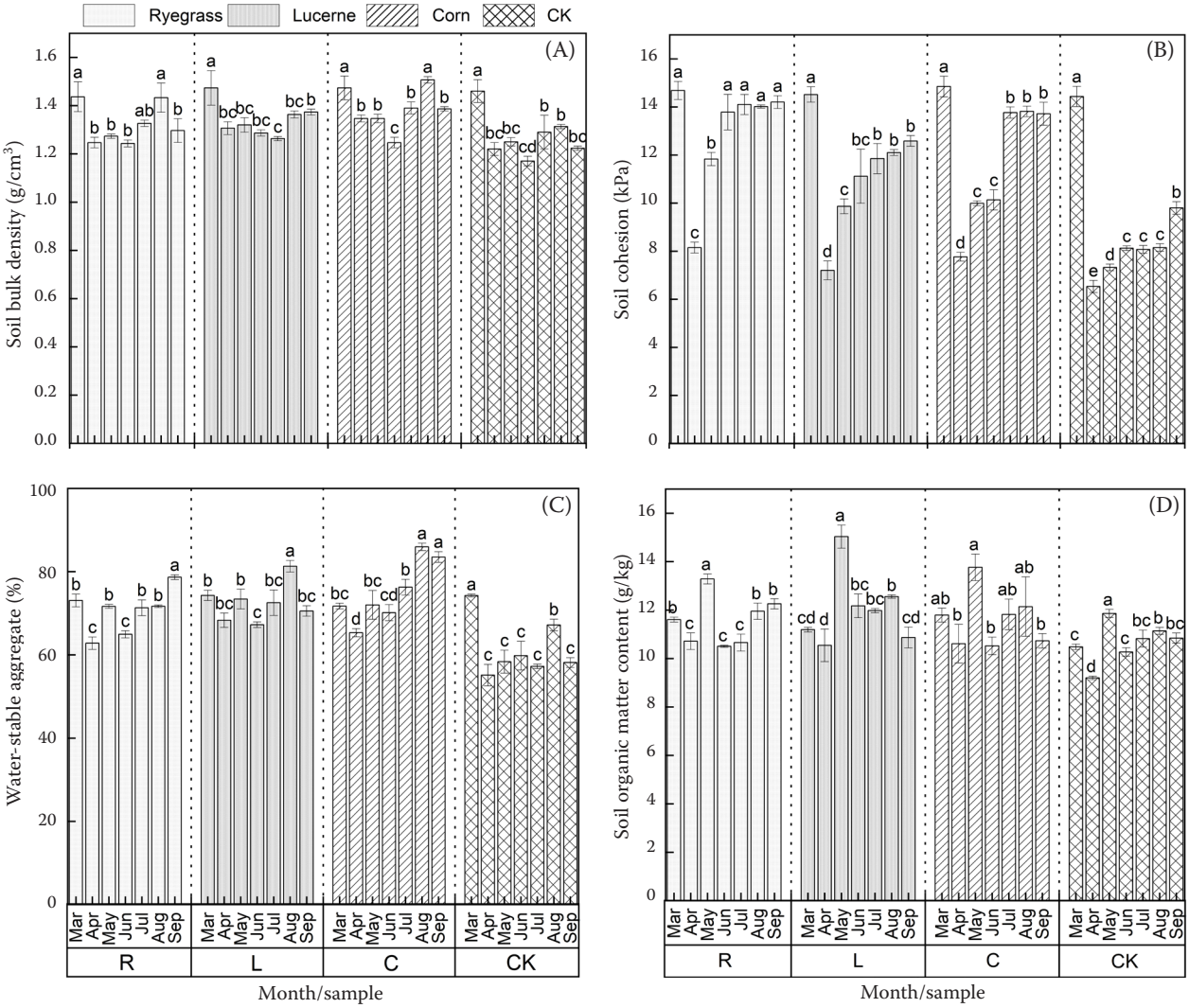

Figure 5. The temporal variation of soil bulk density (A), soil cohesion (B), water-stable aggregate (C), and soil organic matter content (D)

study period. SOC of R, L, C, and CK plots increased by 14.41, 3.06, 1.12 and 17.83%, respectively from April to September.

Root effect. Previous studies have demonstrated that plant cultivation effectively improves the soil erosion (Lu et al. 2012; Berendse et al. 2015). Gyssels et al. (2005) reported that the direct contact of plant roots with the soil is the most critical factor for enhanced resistance to soil erosion. The mechanical action of plant roots and the secreted organic matter can improve the physicochemical properties of the soil. Seitz et al. (2016) suggested that soil physicochemical properties are vital for reducing soil erosion. In this study, K_r and τ_c exhibited a significant correlation with RWD (Table 3). Further, K_r decreased with an increase in RWD, and the relationship between the two can be expressed as a power function with a coefficient of determination of 0.71. In contrast, τ_c increased with an increase RWD, and the relationship between the two can also be expressed as a power function (Figure 6A, B).

RWD of R, L, and C plots increased 1.78, 4.37, and 13.60 times, respectively, from April to September. As shown in Figure 7, the maximum increase in RWD of the R (23.29%) and L (6.19%) plots occurred from April to May. The values of mean K_r in the cropped plots increased in the following order: L (0.0021 g per cm^3) < R (0.0054 g/cm^3) < C (0.0091 g/cm^3). The mean K_r value of C plot was 1.69 and 4.33 times higher than those of R and L plots, respectively.

De Baets et al. (2006) reported that K_r exponentially decreased with an increase in RWD. However, Gys-

https://doi.org/10.17221/42/2023-SWR

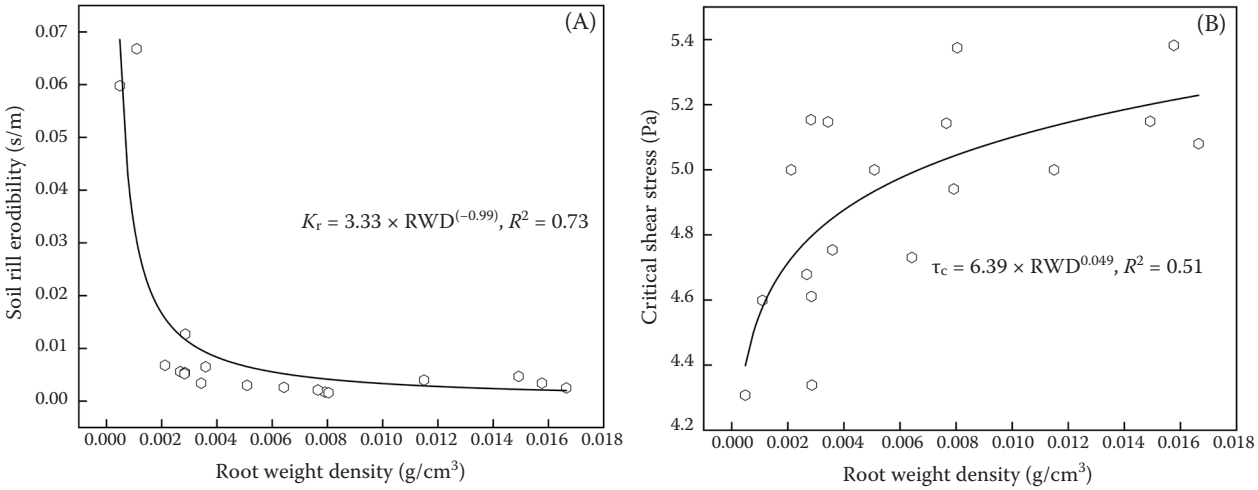

Figure 6. Soil rill erodibility (K_r) (A) and critical shear stress (τ_c) (B) as function of root weight density (RWD)

sels et al. (2006) raised concerns about the rationale behind excluding the influence of other factors on K_r while evaluating the effects of the root system on it. Therefore, the cropland rill adjustment factor of the WEPP soil component (Alberts et al. 1995) can be considered to correct the baseline erodibility factor for the presence of live roots using Equation (4):

$$CK_{lrl} = e^{(-3.5lr)} \quad (4)$$

where:
CK_{lrl} – inter-rill erodibility adjustment;
lr – the mass of the living roots (g/cm^2).

As per the WEPP model, roots should be collected from the top 15 cm of the soil. In this study, RWD was measured based on the top 5 cm of the soil.

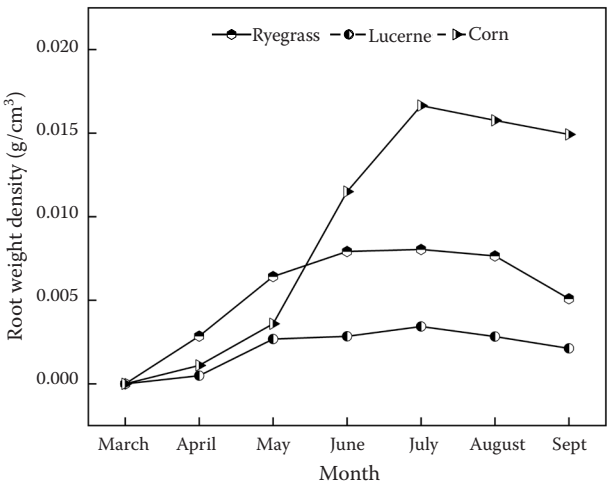

Figure 7. Time variation of root weight density (RWD)

To obtain the K_r adjustment factor, the measured K_r value was normalised by the K_r value under the new tillage conditions. The results obtained in this study were different from those obtained by the WEPP model, with the rate of decline in K_r with increasing RWD overestimated in the WEPP model (Figure 8). This may be attributed to the soil depth chosen for the collection of roots. As mentioned above, the roots were collected from the top 5 cm of the soil in this study, whereas in the WEPP model, roots should be collected from the top 15 cm of the soil. Thus, the K_r value of soil between 5~15 cm depth could not be measured, thereby neglecting the effect of this soil layer on RWD.

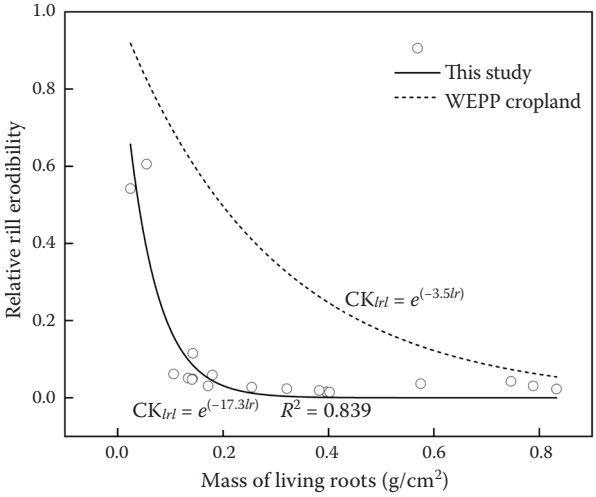

Figure 8. Rill erodibility adjustment factor (CK_{lrl}) for the presence of roots according to water erosion prediction project (WEPP) (dashed line) and the data for conventional ploughing in this study (solid line)

https://doi.org/10.17221/42/2023-SWR

Estimation of soil rill erodibility and critical shear stress

It is challenging to perform the field measurements of K_r and τ_c. Therefore, it is imperative to develop models for predicting K_r and τ_c. The non-linear regression method was used to develop equations for estimating K_r (Equation 5) and τ_c (Equation 6) based on the data on SC and SD. The regression equation, thus obtained, reveal that the variance of K_r and τ_c for all the plots could be explained by SC and SD, with the efficiency of 86.7% and 60.0%, respectively.

$$K_r = 52.342e^{(-0.502SC - 2.316SD)},\ R^2 = 0.867 \quad (5)$$

$$\tau_c = 3.68e^{(0.019SC + 0.052SD)},\ R^2 = 0.600 \quad (6)$$

CONCLUSION

The temporal variation in K_r and τ_c during concentrated flow were investigated for three typical crops (R, L, and C) in western Sichuan of China. The results demonstrated temporal variations in K_r and τ_c in all four plots from April to September. K_r significantly decreased, while τ_c increased in the CK, R, L, and C plots. K_r decreased by 79.20, 91.59, 88.31, and 22.65% for the R, L, C, and CK plots, respectively, from April to May. τ_c, SD, SC, WSA, and SOC were found to be increased by15.25, 4.01, 74.23, 25.27 and 14.41% for the R plot; 16.07, 5.1, 74.77, 3.23 and 3.06% for the L plot; 11.96, 2.97, 76.61, 27.83 and 1.12% for the C plot; 26.60, 0.27, 50, 5.49 and 17.83%, for the CK plot, respectively, from April to September. The temporal variations in K_r and τ_c under different plant species could be explained by the difference in the soil physicochemical parameters such as SD, SC, WSA, SOC, and RWD. K_r showed a strong negative correlation with SD, SC and WSA; and a moderate negative correlation with RWD and SOC. τ_c showed a strong positive correlation with SD, SC and WSA; and a moderate positive correlation with RWD. K_r showed an exponential decline with varying SD, SC, WSA, SOC, and RWD. τ_c increased with an increase in SD, SC, and WSA. The relationship between τ_c and these factors could be expressed as a power function. However, τ_c exponentially increased with an increase in RWD. This study revealed that K_r and τ_c could be accurately estimated from SD (R^2 = 0.867) and SC (R^2 = 0.60).

REFERENCE

Alberts E.E., Nearing M.A., Weltz M.A., Risse L.M., Pierson F.B., Zhang X.C., Laflen J.M., Simanton J.R. (1995): Soil component. Chapter 7. In: Flanagan D.C., Nearing M.A. (eds.): USDA – Water Erosion Prediction Project. Hillslope Profile and Watershed Model Documentation. NSERL Report No. 10. West Lafayette, USDA-ARS National Soil Erosion Research Laboratory.

Amundson R., Berhe A.A., Hopmans J.W., Olson C., Sztein A.E., Sparks D.L. (2015): Soil and human security in the 21st century. Science, 348: 1261071.

Bennett S.J., Casali J., Robinson K.M., Kadavy K.C. (2000): Characteristics of actively eroding ephemeral gullies in an experimental channel. Transactions of the ASAE, 43: 641–649.

Berendse F., Ruijven J.V., Jongejans E., Keesstra S. (2015): Loss of plant species diversity reduces soil erosion resistance. Ecosystems, 18: 881–888.

Bordoloi S., Ng C.W.W. (2020): The effects of vegetation traits and their stability functions in bio-engineered 2 slopes: A perspective review. Engineering Geology, 275: 105742.

Borrelli P., Robinson D.A., Fleischer L.R., Lugato E., Ballabio C., Alewell C., Meusburger K., Modugno S., Schütt B., Ferro V., Bagarello V., Van Oost K., Montanarella L., Panagos P. (2017): An assessment of the global impact of 21st century land use change on soil erosion. Nature Communications, 8: 2013.

De Baets S., Poesen J., Gyssels G., Knapen A. (2006): Effects of grass roots on the erodibility of topsoils during concentrated flow. Geomorphology, 76: 54–67.

Gyssels G., Poesen J., Bochet E., Li Y. (2005): Impact of plant roots on the resistance of soils to erosion by water: A review. Progress in Physical Geography, 29: 189–217.

Gyssels G., Poesen J., Liu G., Van Dessel W., Knapen A., De Baets S. (2006): Effects of cereal roots on detachment rates of single- and double-drilled topsoils during concentrated flow. European Journal of Soil Science, 57: 381–391.

Keesstra S.D., Bouma J., Wallinga J., Tittonell P., Smith P., Cerda A., Montanarella L., Quinton J.N., Pachepsky Y., Putten W.H.D., Bardgett R., Moolenaar S., Mol G., Jansen B.O., Freco L. (2016): The significance of soils and soil science towards realization of the United Nations Sustainable Development Goals. Soil, 2: 111–128.

Knapen A., Poesen J., De Baets S. (2007a): Seasonal variations in soil erosion resistance during concentrated flow for a loess-derived soil under two contrasting tillage practices. Soil & Tillage Research, 94: 425–440.

Knapen A., Poesen J., Govers G., Gyssels G., Nachtergaele J. (2007b): Resistance of soils to concentrated flow erosion: A review. Earth-Science Reviews, 80: 75–109.

https://doi.org/10.17221/42/2023-SWR

Li Z., Fang H. (2016): Impacts of climate change on water erosion: A review. Earth-Science Reviews, 163: 94–117.

Lu Y.H., Fu B.J., Feng X.M., Zeng Y., Liu Y., Chang R.Y., Sun G., Wu B.F. (2012): A policy-driven large scale ecological restoration: Quantifying ecosystem services changes in the loess plateau of China. PLoS ONE, 7: e31782.

Mamo M., Bubenzer G.D. (2001a): Detachment rate, soil erodibility, and soil strength as influenced by living plant roots. Part I: Laboratory study. Transactions of the ASAE, 44: 1167–1174.

Mamo M., Bubenzer G.D. (2001b): Detachment rate, soil erodibility, and soil strength as influenced by living plant roots. Part II: Field study. Transactions of the ASAE, 44: 1175–1181.

Maetens W., Poesen J., Vanmaercke M. (2012): How effective are soil conservation techniques in reducing plot runoff and soil loss in Europe and the Mediterranean? Earth-Science Reviews, 115: 21–36.

Minasny B., Brendan P.M., Alex B.M., Angers D.A., Arrouays D., Chambers A., Chaplot V., Chen Z.S., Cheng K., Bas B.S., Field D.J., Gimona A. (2017): Soil carbon 4 per mille. Geoderma, 292: 59–86.

Nearing M.A., Foster G.R., Lane L.J., Finkner S.C. (1989): A process-based soil erosion model for USDA – Water erosion prediction project technology. Transactions of the ASAE, 32: 1587–1593.

Norris J.E. (2005): Root reinforcement by hawthorn and oak roots on a highway cut-slope in southern England. Plant & Soil, 278: 43–53.

Seitz S., Goebes P., Song Z., Bruelheide H., Hardtle W., Kuhn P., Li Y., Scholten T. (2016): Tree species and functional traits but not species richness affect interrill erosion processes in young subtropical forests. Soil, 2: 49–61.

Six J., Paustian K., Elliott E.T., Combrink C. (2000): Soil structure and organic matter I. Distribution of aggregate-size classes and aggregate-associated carbon. Soil Science Society of America Journal, 64: 681–689.

Stokes A., Douglas G.B., Fourcaud T., Giadrossich F., Gillies C., Hubble T., Kim J H. (2014): Ecological mitigation of hillslope instability: Ten key issues facing researchers and practitioners. Plant Soil, 377: 1–23.

Sun L., Zhang G.H., Liu F., Luan L.L. (2016): Effects of incorporated plant litter on soil resistance to flowing water erosion in the Loess Plateau of China. Biosystems Engineering, 147: 238–247.

Virto I., Gartzia B.N., Fernandez-Ugalde O. (2011): Role of organic matter and carbonates in soil aggregation estimated using laser diffractometry. Pedosphere, 21: 566–572.

Wang B., Zhang G.H., Shi Y.Y., Zhang X.C. (2014a): Soil detachment by overland flow under different vegetation restoration models in the Loess Plateau of China. Catena, 116: 51–59.

Wang B., Zhang G.H., Zhang X.C., Zhen W.L., Su Z.L., Yi T., Shi Y.Y. (2014b): Effects of near soil surface characteristics on soil detachment by overland flow in a natural succession grassland. Soil Science Society of America Journal, 78: 589–597.

Wang H., Zhang G.H., Liu F., Geng R., Wang L.J. (2017): Effects of biological crust coverage on soil hydraulic properties for the Loess Plateau of China. Hydrological Processes, 31: 3396–3406.

Wang H., Zhang G.H., Li N.N., Zhang B.J., Yang H.Y. (2018): Soil erodibility influenced by natural restoration time of abandoned farmland on the Loess Plateau of China. Geoderma, 325: 18–27.

Wang J., Huang J., Wu P., Zhao X., Gao X.D., Dumlao M., Bing C.S. (2015): Effects of soil managements on surface runoff and soil water content in jujube orchard under simulated rainfalls. Catena, 135: 193–201.

Wen Y.C., Xue X.X, Ruo H. (2017): Effects of forestlands and grasslands on soil aggregates under different vegetation restoration ages in loess hilly region. Acta Scientiae Circumstantiae, 37: 1486–1492.

Yu Y.C., Zhang G.H., Geng R., Li Z.W. (2014): Temporal variation in soil rill erodibility to concentrated flow detachment under four typical croplands in the Loess Plateau of China. Journal of Soil and Water Conservation, 69: 352–363.

Zhang B.J., Zhang G.H., Yang H.Y., Wang H. (2019a): Soil resistance to flowing water erosion of seven typical plant communities on steep gully slopes on the Loess Plateau of China. Catena, 173: 375–383.

Zhang B.J., Zhang G.H., Yang H.Y., Zhu P.Z. (2019b): Temporal variation in soil erosion resistance of steep slopes restored with different vegetation communities on the Chinese Loess Plateau. Catena, 182: 104170.

Zhang G.H., Tang K.M., Ren Z.P., Zhang X.C. (2013): Impact of grass root mass density on soil detachment capacity by concentrated flow on steep slopes. Transactions of the ASABE, 56: 927–934.

Zhao G., Mu X., Wen Z., Wang F., Gao P. (2013): Soil erosion, conservation, and eco-environment changes in the Loess Plateau of China. Land Degradation & Development, 24: 499–510.

Zhen W.L., Zhang G.H., Geng R., Wang H. (2015): Rill erodibility as influenced by soil and land use in a small watershed of the Loess Plateau, China. Biosystems Engineering, 129: 248–257.

Zhou H., Peng X., Peth S., Xiao T.Q. (2012): Effects of vegetation restoration on soil aggregate microstructure quantified with synchrotron-based micro-computed tomography. Soil and Tillage Research, 124: 17–23.

Received: May 6, 2023
Accepted: July 21, 2023
Published online: July 31, 2023